

THE PHYSICAL REVIEW

A journal of experimental and theoretical physics established by E. L. Nichols in 1893

SECOND SERIES, VOL. 187, No. 1

5 NOVEMBER 1969

Widths of the $K\alpha_1$ and $K\alpha_2$ X-Ray Lines for $Z > 50^\dagger$

G. C. Nelson, W. John, and B. G. Saunders

Lawrence Radiation Laboratory, University of California, Livermore, California 94550

(Received 11 August 1969)

A Cauchois-type transmission bent-crystal spectrometer has been used to measure the full width at half-maximum of the $K\alpha_1$ and $K\alpha_2$ x rays of 36 elements from $_{51}\text{Sb}$ to $_{95}\text{Am}$. The x-ray lines were fitted by folding a Lorentzian natural line shape with a Gaussian instrumental response and integrating over the detector-slit width. The present results are systematically somewhat higher than the values deduced from recent theoretical calculations of the radiative widths and the appropriate experimental fluorescent yields.

INTRODUCTION

For the last 40 years, experiments have been carried out to determine the atomic level widths and the natural x-ray widths. Most of the work on $K\alpha_1$ and $K\alpha_2$ x-ray widths¹⁻⁴ has been concentrated on elements below $_{50}\text{Sn}$. There have been some measurements made of the widths of L x-ray lines of heavier elements.

Recently, Scofield⁵ has used the relativistic Hartree-Slater potential to calculate the radiative widths for the K and L shells for elements $_{13}\text{Al}$ to $_{92}\text{U}$. Since the fluorescent yield for a given shell is defined as the radiative width divided by the total width, the total K and L widths can be determined by dividing the K - and L -shell radiative widths by the appropriate fluorescent yields. The $K\alpha_1$ and $K\alpha_2$ x-ray widths are then obtained by adding, respectively, the total L_{111} and L_{11} widths to the total K width. These values can then be compared with the experimentally measured $K\alpha_1$ and $K\alpha_2$ x-ray widths.

The purpose of the present experiment was to systematically measure the widths of the $K\alpha_1$ and $K\alpha_2$ x-rays for elements $_{51}\text{Sb}$ to $_{95}\text{Am}$ and to compare these results with the values deduced from the radiative widths calculated by Scofield⁵ and the appropriate fluorescent yields.

EXPERIMENTAL METHOD

K x rays from heavy elements have lifetimes on the order of 10^{-17} sec, which corresponds to natural widths of tens of electron volts. Because the resolution of double-crystal and bent-crystal spectrometers is of the same order as the natural x-ray widths, these spectrometers are used to measure x-ray widths. The major difficulty in these measurements is the proper correction for the instrumental response. The observed distribution of energy through the x-ray line $f(\nu)$ is given by

$$f(\nu) = \int_{-\infty}^{\infty} \psi(\nu') \phi(\nu - \nu') d\nu', \quad (1)$$

where ψ is the true distribution and ϕ is the instrumental response. Various attempts have been made to correct the observed spectra for the instrumental response. These vary from empirical corrections such as $W_{\text{obs}} = W_T + W_I/2$,⁶ where W_T is the true width and W_I is the instrumental width, to assumptions about the form of ψ and ϕ such that Eq. (1) can easily be solved. One of the earliest attempts of this latter method was to assume that both the instrumental response and the natural shape are Gaussians. When Eq. (1) is solved with these assumptions one is led to the

Schwarzschild⁷ equation, $W_{\text{obs}}^2 = W_T^2 + W_I^2$. However, investigators found that the experimentally determined line profile did not follow the Gaussian shape. Weisskopf and Wigner⁸ have shown that the natural shape should have the Lorentzian form

$$\psi(\nu) = A / [(\nu - \nu_0)^2 + (\frac{1}{2}\Gamma)^2],$$

where ν is the frequency of the radiation, ν_0 is the frequency of the center of the peak, and Γ is the full width at half-maximum (FWHM) of the line. Using this Lorentzian function for the natural line shape and assuming the instrumental response is of the same form, one is led to the Hoyt⁹ equation, $W_{\text{obs}} = W_T + W_I$. It has been experimentally determined³ that the assumption of a Lorentzian shape for both the instrumental response and the natural x-ray shape gives a good fit to the experimental data obtained with double-crystal spectrometers.

Because its efficiency is higher than that of a double-crystal spectrometer, it is desirable to use a bent-crystal spectrometer to measure the widths of high Z elements. In this case, the instrumental profile does not follow the Lorentzian shape. In the present measurements it was determined that the instrumental profile could be fitted very well by a Gaussian shape. With the assumption of a Gaussian shape for the instrumental profile and Lorentzian shape for the natural x-ray distribution, we have solved Eq. (1) numerically on a CDC 3600 computer and have used the function $f(\nu)$ to fit our experimental data.

The 2-m Cauchois-type transmission bent-crystal spectrometer used in the present measurements is described in Ref. 10, and the source arrangement is described in Ref. 11. The 2.5- by 7.5-cm targets were placed at a 45° angle with respect to a 50-Ci ¹⁸²Ta source. The Ta source was shielded from the diffraction crystal. The fluoresced x rays were diffracted by the (310) planes of a 2-mm-thick quartz crystal. The diffracted rays converged at the detector slit and were recorded in a 2-cm³ thin window Ge(Li) detector.

The diffracted x-ray peak shapes were determined by automatically stepping the 0.176-mm-wide detector slit 200 steps of 0.01 mm each across the diffraction peaks. The counting time per step varied from 2 to 15 min, depending on the intensity of the line being studied. A single-channel analyzer was used to select the energy region of interest.

The instrumental profile was determined by measuring the profiles of four γ rays in the energy range of 59 to 100 keV. Gamma rays have natural widths which are negligible in comparison to the instrumental width. The observed γ -ray line profile was assumed to be a fold of a Gaussian instrumental shape into the detector slit. The resulting function was then fit to the experimental data. The fitting procedure is described in Ref. 10. Figure 1

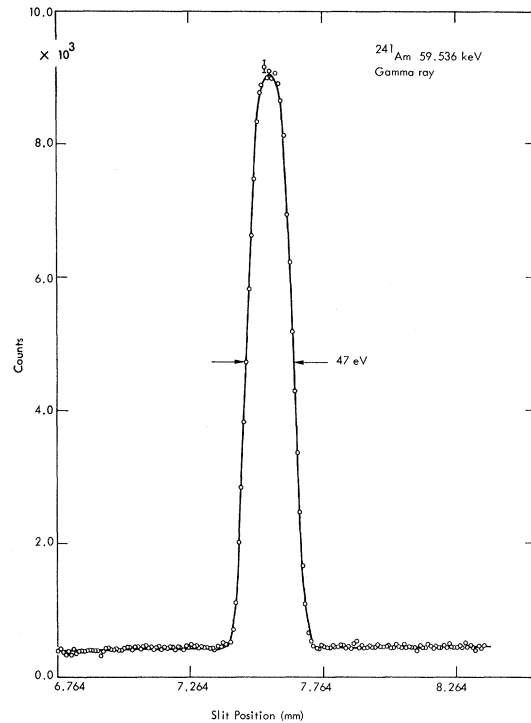


FIG. 1. Least-squares computer fit to the 59.536-keV Am^{241} γ -ray diffraction peak.

is a computer fit to the 59.536-keV ²⁴¹Am γ ray. It can be seen that the assumption of a Gaussian distribution for the instrumental profile gives an excellent fit to the data. In the present experiment it was found that in the energy range of 59 to 100 keV the instrumental width remained constant to within 1%. This is in agreement with the observation of Edwards¹² that the instrumental width is not a function of energy.

In the present x-ray measurements, it was assumed that the natural x-ray shape was Lorentzian and the instrumental response was Gaussian. The observed spectrum was obtained by folding these functions into the detector slit. A linear background was also assumed. The experimental data were fitted with the function

$$y(x_i) = A + Bx_i + C \int_{x_i - \frac{1}{2}S}^{x_i + \frac{1}{2}S} \frac{e^{-4\ln 2(\xi/\sigma)^2}}{(u - x_0 + \xi)^2 + (\frac{1}{2}\Gamma)^2} d\xi du, \quad (2)$$

where σ is the FWHM of the instrumental response, x_0 is the center of the diffraction peak, Γ is the natural width of the x ray, S is the slit width, x_i is the slit position, and $y(x_i)$ is the counting rate at position x_i . Figure 2 is a computer fit of Eq. (2) to the Ir $K\alpha_1$ x ray. The successful fit can be

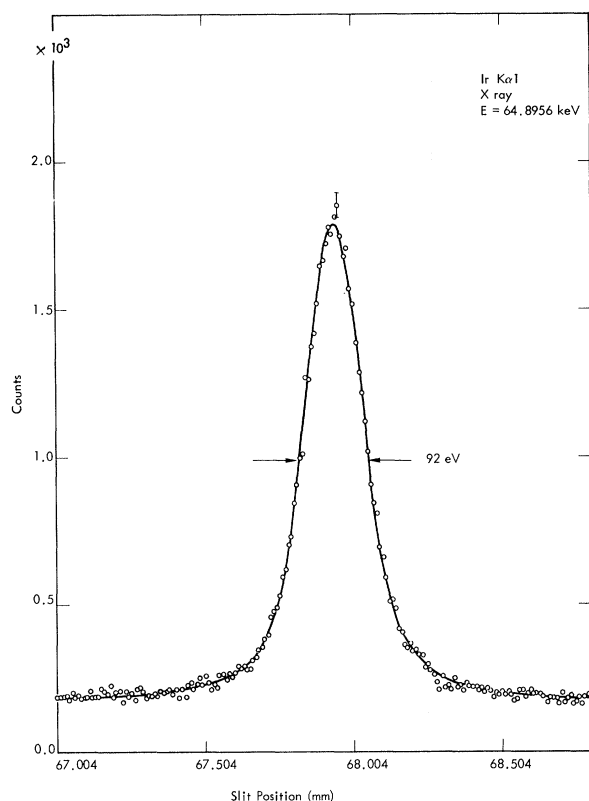


FIG. 2. Least-squares computer fit to the Ir $K\alpha_1$ x-ray diffraction peak.

considered as confirmation of the proper choice of natural line shape.

The x-ray width in eV was determined from Γ , the width in millimeters, by differentiating the position-versus-energy calibration curve, $x_0 = 10.607/E + B$. This gave

$$\Delta E = (\Gamma/10.607)E^2, \quad (3)$$

where E is in keV and ΔE is in eV. The x-ray energies for elements below Np were taken from Bearden¹³ while the values for the transuranic elements Np, Pu, and Am were those reported by the present authors in Ref. 11.

RESULTS AND DISCUSSION

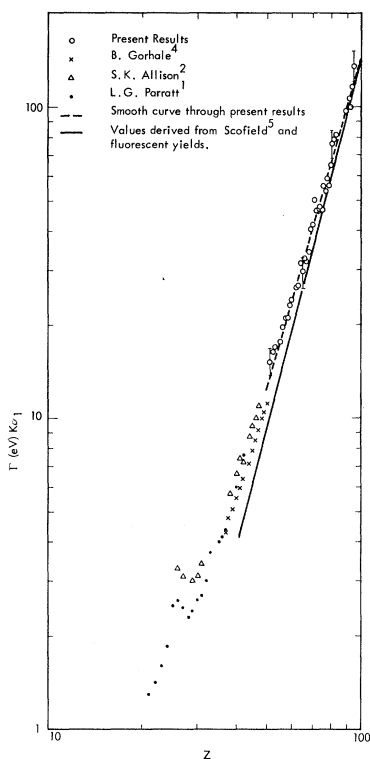
Table I lists the measured $K\alpha_1$ and $K\alpha_2$ widths for 36 elements between ${}_{51}\text{Sb}$ and ${}_{95}\text{Am}$. The estimated errors of 10% are due to the uncertainty introduced by the slit width, the instrumental width, and the statistical uncertainty in the data. The error introduced by the uncertainty in the slit width and the uncertainty in the instrumental width is approximately equal to the statistical uncertainty.

In Figs. 3 and 4 are plotted the $K\alpha_1$ and $K\alpha_2$ widths obtained in the present experiments. The

previous data of Parratt,¹ Allison,² and Richtmyer and Barnes³ obtained with double-crystal spectrometers, and the data of Gokhale⁴ obtained with a bent-crystal spectrometer, are plotted for comparison. The solid curves are semitheoretical values, which were obtained by dividing Scofield's⁵ theoretical total radiative widths for the K , L_{11} , and L_{111} shells by the appropriate fluorescent yields to obtain the total level widths. The fluorescent yields of Wapstra *et al.*¹⁴ were used for the K shell, and the measurements of Price *et al.*¹⁵

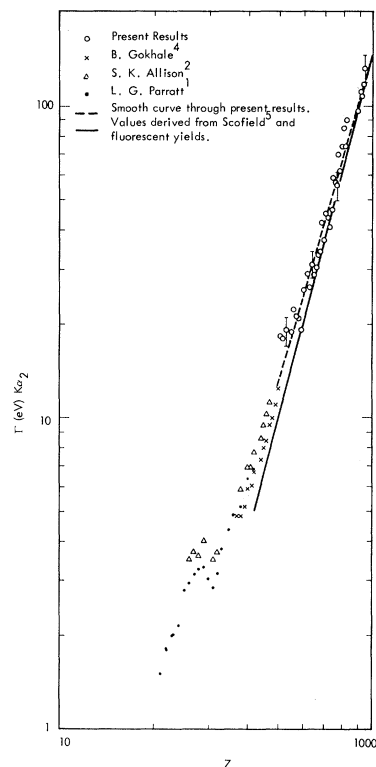
TABLE I. The measured $K\alpha_1$ and $K\alpha_2$ x-ray line-widths for elements ${}_{51}\text{Sb}$ to ${}_{95}\text{Am}$. Estimated errors are $\pm 10\%$.

Element	Width (eV)	
	$K\alpha_1$	$K\alpha_2$
${}_{95}\text{Am}$	135.0	130.4
${}_{94}\text{Pu}$	115.7	116.4
${}_{93}\text{Np}$	97.8	106.5
${}_{92}\text{U}$	106.8	109.0
${}_{90}\text{Th}$	96.1	95.5
${}_{83}\text{Bi}$	80.8	89.1
${}_{82}\text{Pb}$	77.9	73.9
${}_{81}\text{Tl}$	75.9	84.0
${}_{80}\text{Hg}$	64.7	74.0
${}_{79}\text{Au}$	55.6	61.2
${}_{78}\text{Pt}$	58.7	69.1
${}_{77}\text{Ir}$	53.1	55.1
${}_{76}\text{Os}$	55.2	56.1
${}_{75}\text{Re}$	46.5	58.5
${}_{74}\text{W}$	47.5	46.2
${}_{73}\text{Ta}$	46.5	40.5
${}_{72}\text{Hf}$	46.3	43.4
${}_{71}\text{Lu}$	50.0	44.9
${}_{70}\text{Yb}$	41.5	36.7
${}_{69}\text{Tm}$	40.3	42.0
${}_{68}\text{Er}$	34.0	33.8
${}_{67}\text{Ho}$	31.9	33.3
${}_{66}\text{Dy}$	32.5	30.2
${}_{65}\text{Tb}$	29.5	28.7
${}_{64}\text{Gd}$	31.5	30.9
${}_{63}\text{Eu}$	26.1	26.2
${}_{62}\text{Sm}$	26.3	28.8
${}_{60}\text{Nd}$	23.8	25.5
${}_{59}\text{Pr}$	23.0	19.2
${}_{58}\text{Ce}$	21.0	20.9
${}_{57}\text{La}$	21.0	21.1
${}_{56}\text{Ba}$	19.6	22.2
${}_{55}\text{Cs}$	17.5	18.8
${}_{53}\text{I}$	16.8	19.1
${}_{52}\text{Te}$	16.4	17.9
${}_{51}\text{Sb}$	15.2	18.3

FIG. 3. FWHM of the $K\alpha_1$ rays as a function of Z .

were used for the L_{11} and L_{111} shells. The $K\alpha_1$ and $K\alpha_2$ x-ray widths were then obtained by adding the total L_{111} and L_{11} widths, respectively, to the total K width. The dashed lines in Figs. 3 and 4 are smooth curves drawn through the present data points. These lines vary as $Z^{3.47}$, whereas the lines derived from the calculations of Scofield vary as $Z^{3.87}$. The experimental and calculated lines intersect at $Z \approx 100$. The dashed lines, when extended to lower atomic numbers, fall between the data of Allison² and that of Gokhale.⁴ It should be noted that Allison's data are uncorrected for instrumental effects, while Gokhale has corrected for the instrumental width. The present values for the widths of the ^{74}W lines are 7 to 10% higher than the measured values of Richtmyer and Barnes,³ but the difference is within the experimental error.

It is apparent that the present data trend away from the theoretical curve as Z decreases. This

FIG. 4. FWHM of the $K\alpha_2$ x rays as a function of Z .

trend continues through the older data at lower Z . The reason for the different Z dependence of experiment and theory is at present not understood.

SUMMARY

Measurements of the $K\alpha_1$ and $K\alpha_2$ x-ray line-widths have been made for 36 elements between ^{51}Sb and ^{95}Am for the first time. The observed widths have been corrected for the broadening introduced by the instrumental resolution. The present results follow a $Z^{3.47}$ curve, and are systematically somewhat higher than the values obtained from the total radiative widths recently calculated by Scofield.⁵

ACKNOWLEDGMENT

The authors wish to thank J. H. Scofield for his helpful discussions.

[†]Work performed under the auspices of the U. S. Atomic Atomic Energy Commission.

¹L. G. Parratt, Phys. Rev. **50**, 1 (1936).

²S. K. Allison, Phys. Rev. **44**, 63 (1933).

³F. K. Richtmyer and S. W. Barnes, Phys. Rev. **46**, 352 (1934).

⁴B. Gokhale, Ann. Phys. **7**, 852 (1952).

⁵J. H. Scofield, Phys. Rev. **179**, 9 (1969).

⁶F. K. Richtmyer, S. W. Barnes, and E. Ramberg, Phys. Rev. **46**, 853 (1934).

⁷M. M. Schwarzschild, Phys. Rev. **32**, 162 (1928).

⁸V. Weisskopf and E. Wigner, Z. Physik **63**, 54 (1930).

- ⁹A. Hoyt, Phys. Rev. 40, 477 (1932).
¹⁰R. W. Jewell, W. John, R. Massey, and B. G. Saunders, Nucl. Instr. Methods 62, 68 (1968). The "pedestal" on the γ -ray line shape mentioned in Ref. 10 has since been traced to a slit edge-penetration effect and has been eliminated by a simple modification of the slit.
¹¹G. C. Nelson, B. G. Saunders, and W. John, University of California Radiation Laboratory, Report No. UCRL-71746 (report prior to publication).
¹²W. F. Edwards, Ph.D. thesis, California Institute of Technology, Pasadena, Calif., 1960 (unpublished).
¹³J. A. Bearden, Rev. Mod. Phys. 39, 78 (1967).
¹⁴A. H. Wapstra, G. J. Nijgh, and R. van Lieshout, Nuclear Spectroscopy Tables (North-Holland Publishing Co., Amsterdam, 1959).
¹⁵R. E. Price, H. Mark, and C. D. Swift, Phys. Rev. 176, 3 (1968).

Hyperfine Structure of the Ground State of ${}^3\text{He}^+$ by the Ion-Storage Exchange-Collision Technique*

H. A. Schuessler,† E. N. Fortson, and H. G. Dehmelt

Department of Physics, University of Washington, Seattle, Washington 98105

(Received 13 March, 1969)

The hfs of the ground state of ${}^3\text{He}^+$ has been studied using the spin-dependent collision processes between stored ${}^3\text{He}^+$ ions and a polarized beam of Cs atoms. All possible hfs transitions have been measured in a magnetic field of about 7.13 G. A consecutive-pulse multiple-resonance scheme was developed to detect the only weakly field-dependent transition ($F=0$, $m_F=0$) \leftrightarrow ($F=1$, $m_F=0$) in an almost ideally isolated and pure atomic system. Magnetic-resonance disorientation is observed as a change in the number of ions remaining in the rf quadrupole ion trap after a fixed interaction time with both the resonant rf fields and the polarized atomic beam. For the detection of an ion-number signal, the ion macromotion at $\bar{\omega}_z$ was coherently excited by a homogeneous electric field at $\bar{\omega}_z + \Omega$, where Ω is the frequency of the inhomogeneous rf field used for trapping. Linewidths of 10 Hz have been measured for the (0,0) \leftrightarrow (1,0) hfs transition, when the transition was induced during a time of the order of half the electron-spin orientation time in a weak atomic beam. The value for the zero-magnetic-field hfs splitting is $\Delta\nu = (8\,665\,649\,867 \pm 10)$ Hz. Rate equations for the populations of the hfs Zeeman levels in the presence of the polarized atomic beam and transitions caused by various rf fields are given. Features of the line shape caused by the consecutive-pulse multiple-resonance scheme are also considered. Several mechanisms which may ultimately limit the precision are discussed. A comparison of the experimental result with current theories of the hfs of hydrogenic systems is presented.

OUTLINE

- | | |
|---|---|
| I. Introduction | C. Cesium Beam |
| II. Theory of the Experiment | D. Magnetic Field |
| A. hfs of the $1s^2S_{1/2}$ Ground State | E. Ion Trap Electronics |
| B. Spin-Dependent Collision Processes | F. Microwave Generation and Stabilization |
| C. Consecutive-Pulse Multiple-Resonance Scheme | G. Spectral Purity |
| D. Rate Equations | H. Frequency Measurement |
| E. Line-Shape Considerations and Transition Probabilities | I. Microwave Field Geometry |
| F. Electrodynamic Ion Storage | IV. Manipulation of Stored Charge |
| III. Apparatus | A. Excitation of Coherent Ion Motion |
| A. Vacuum System | B. Detection of the Ion-Number Signal |
| B. Ion Storage | C. Effect of the Ion Space Charge |
| | V. Measurements |
| | A. Detection Procedure |
| | B. Results |